Supplementary Information

One-Step Synthesis of Carbon-Supported Pd@Pt/C Core-Shell Nanoparticles as Oxygen Reduction Electrocatalysts and Their Enhanced Activity and Stability

Yuntaek Lim, Seok Ki Kim, Seung-Cheol Lee, Junghun Choi, Kee Suk Nahm, and Sung Jong Yoo,* and Pil Kim*

*To whom correspondence should be addressed. E-mail: ysj@kist.re.kr, kimpil1@chonbuk.ac.kr

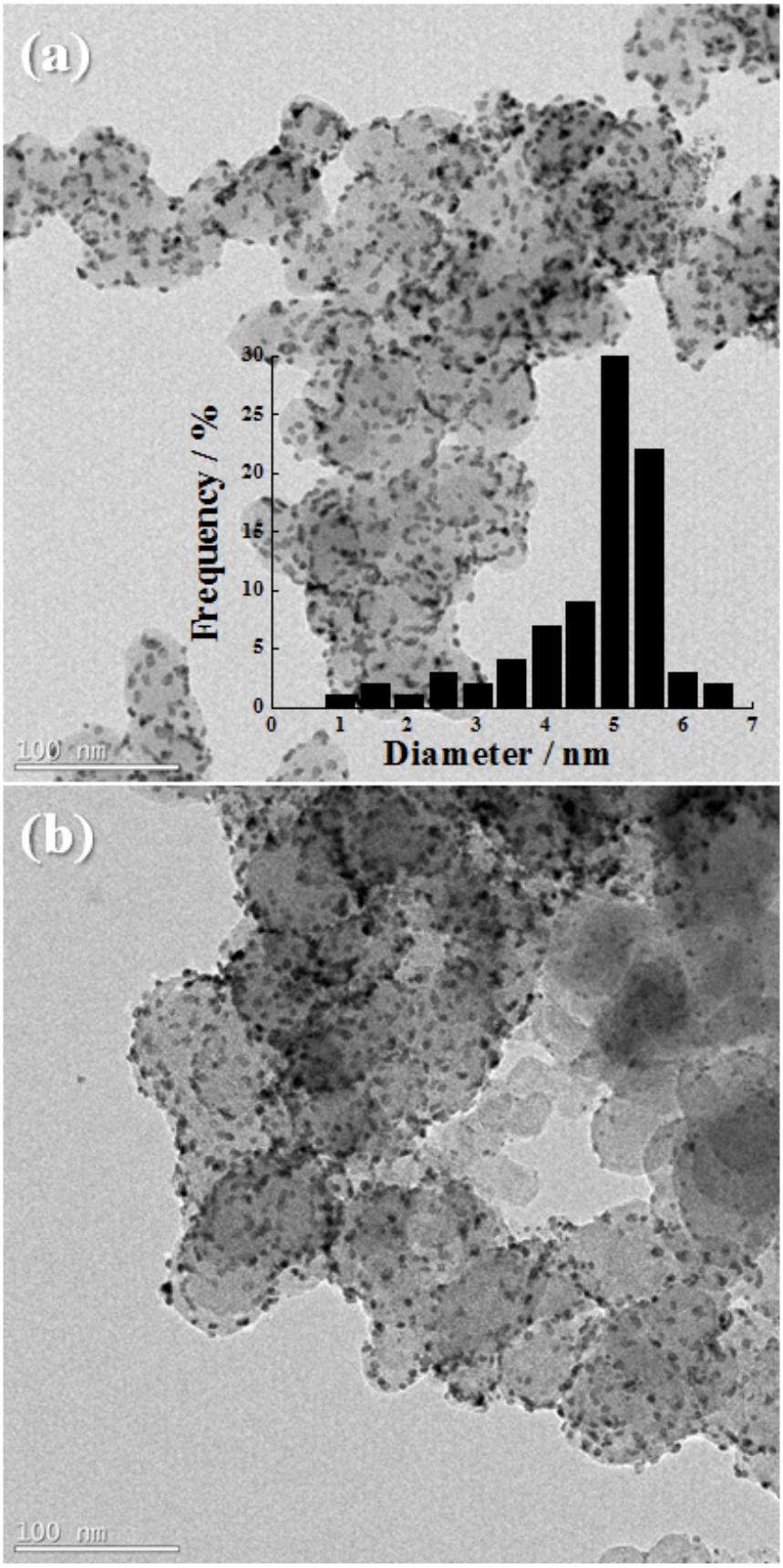

Fig. S1. TEM images of Pd@Pt/C core-shell nanoparticles.

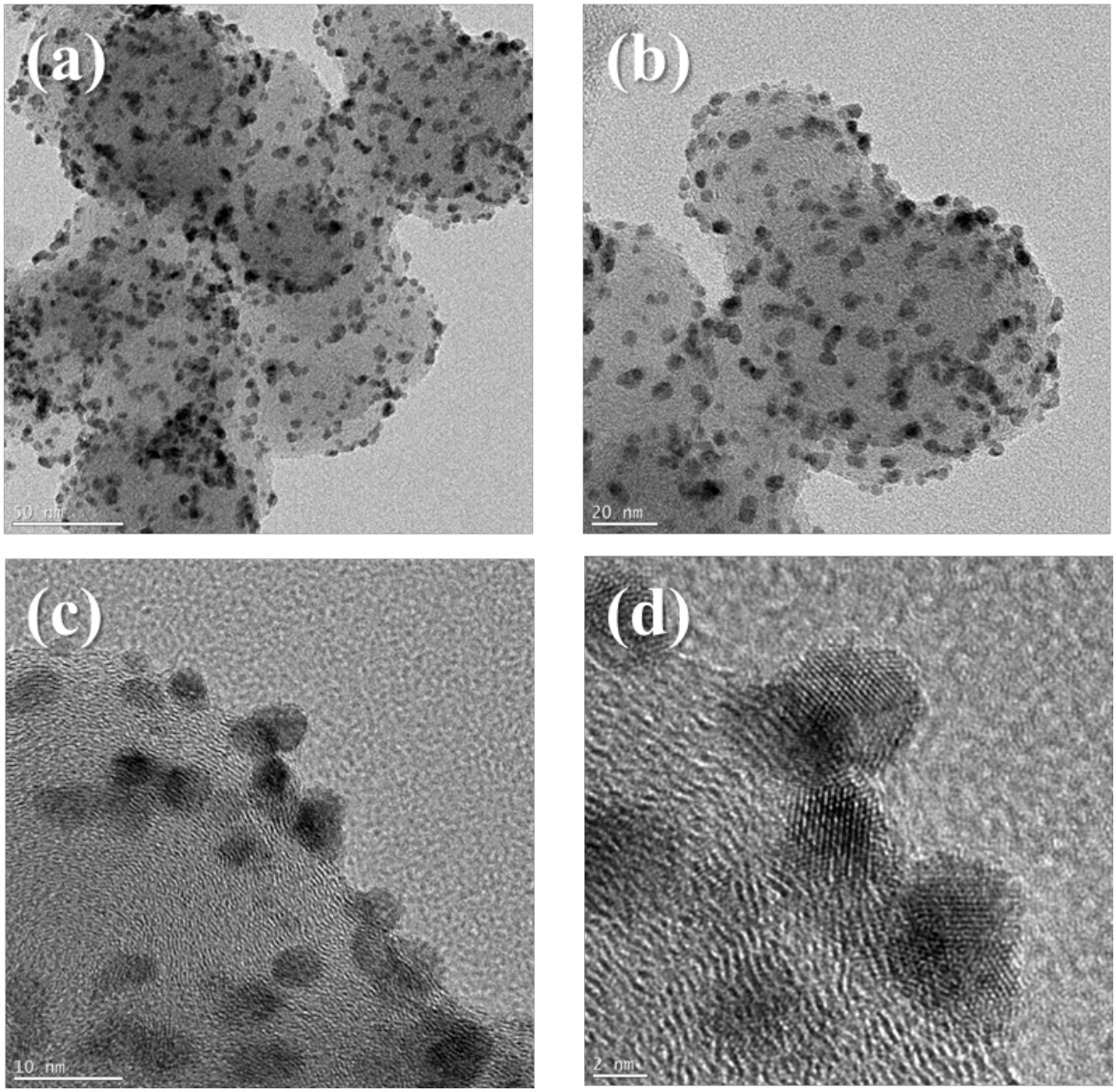

Fig. S2. High-resolution TEM images of Pd@Pt/C core-shell nanoparticles.

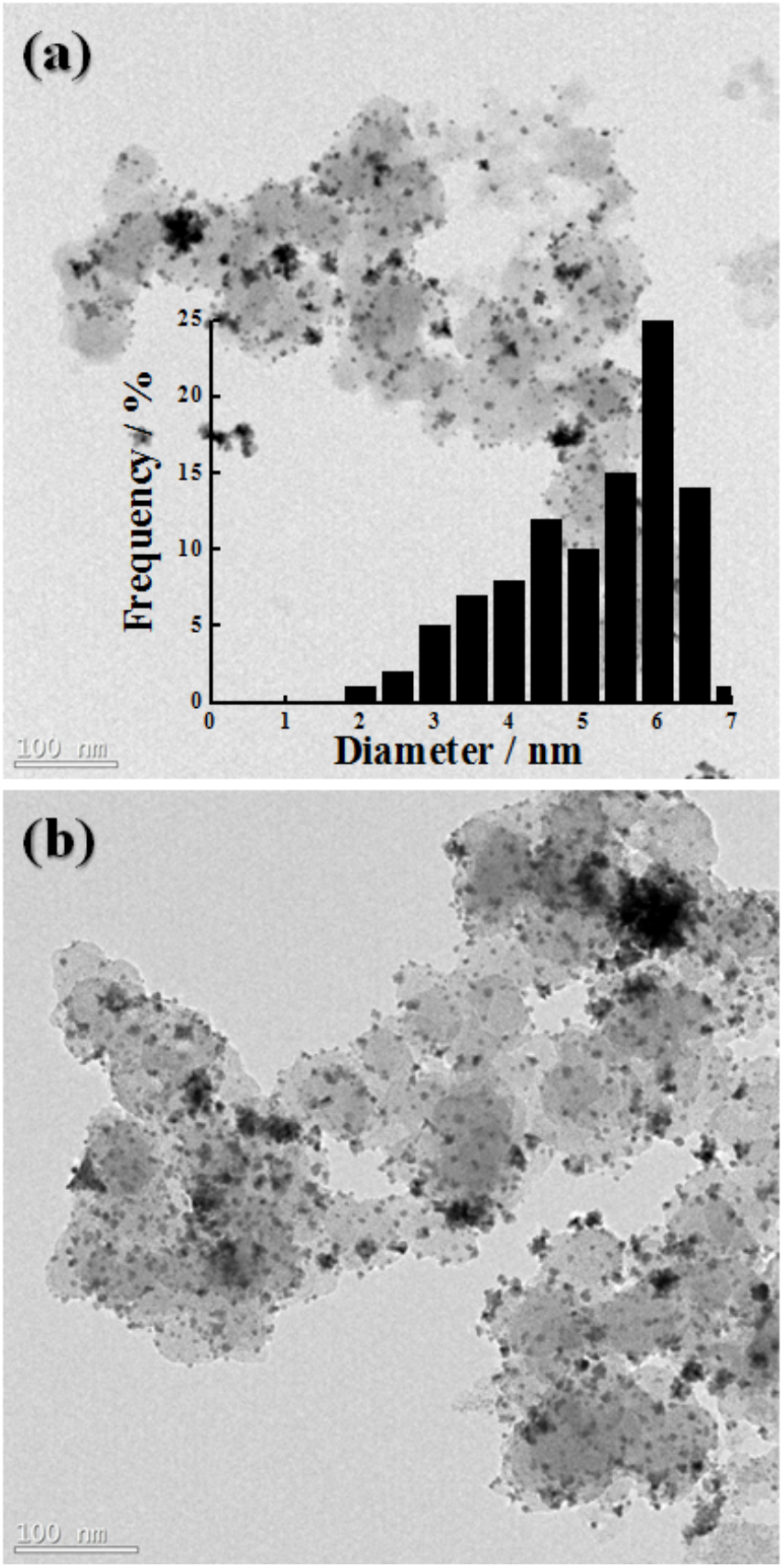

Fig. S3. TEM images of PdPt/C alloy nanoparticles.

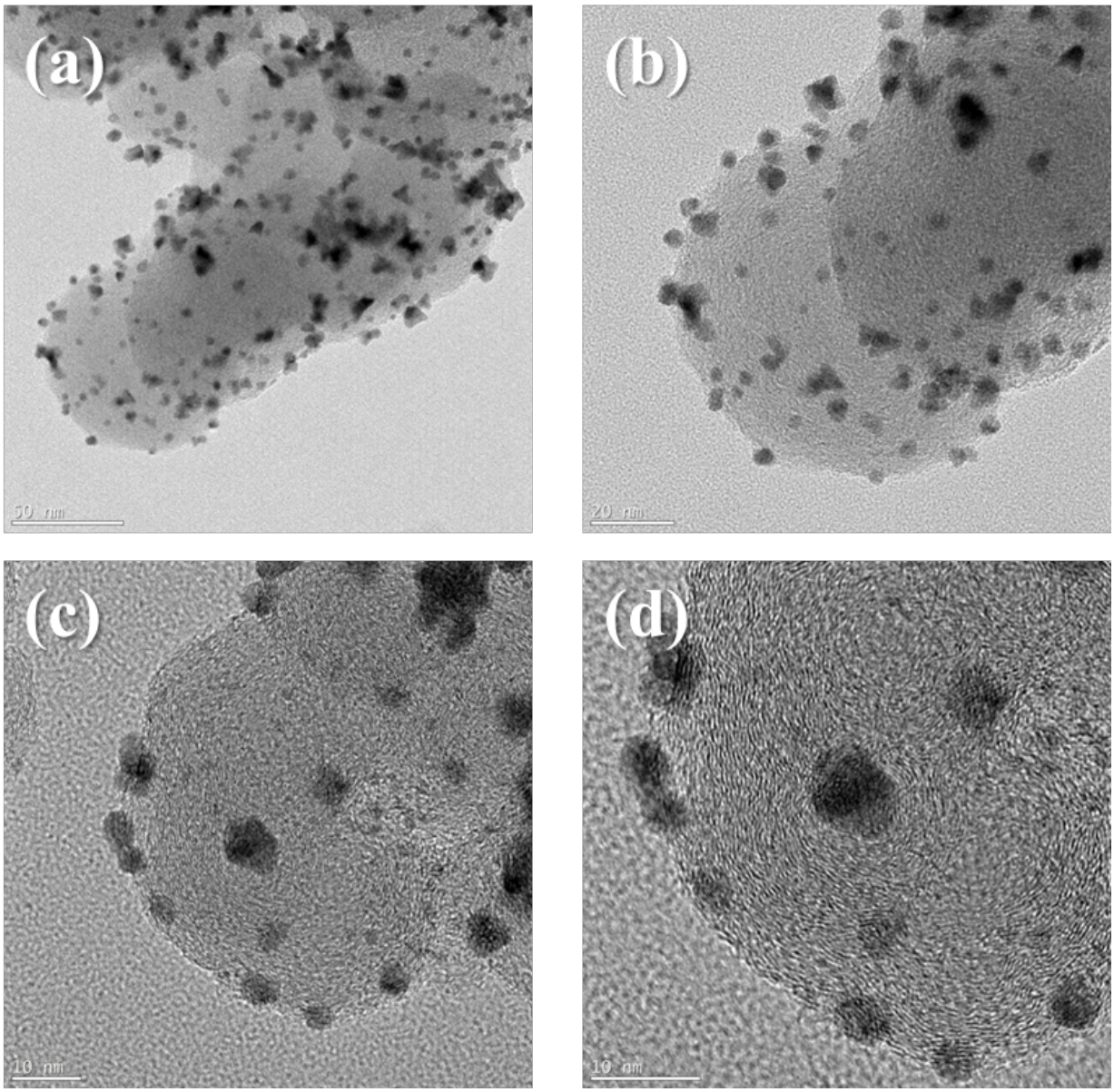

Fig. S4. High-resolution TEM images of PdPt/C alloy nanoparticles.

Table S1. Data on the surface compositions of the PdPt/C alloy and Pd@Pt/C core-shell nanoparticles using selective reduction of carbon dioxide adsorbed by Pt.

Samples	Q_{CO} (mC/mg)	Q_{CO2} (mC/mg)	Q_{CO2}/Q_{CO} (%)	Relative coverage (%)
Pt/C	243.5	95.1	39	100
PdPt/C alloy	268.2	43.9	16	42
Pd@Pt/C core-shell	196.4	65.9	34	86

1. Synchrotron X-ray absorption spectroscopy

To evaluate the local structure of core-shell nanoparticles, we measured X-ray absorption spectroscopy (XAS) on carbon-supported Pd@Pt/C core-shell nanoparticles. XAS experiments were conducted on 5A beamline of Pohang Accelerator Laboratory (PAL) (2.5 GeV; 150-180 mA). The incident beam was monochromatized using a Si(111) double crystal monochromator and detuned by 30% to minimize the contamination from higher harmonics, in particular, the third order reflection of the silicon crystals. The spectra for L_{III}-edge of Pt (E_0 =11564 eV) were taken in a transmission mode with separate He-filled IC Spec ionization chambers for incident and transmitted beams, respectively. Before measuring samples, energy was calibrated by using of Pt foil. The energy scan was performed in five regions for good energy resolution in a steep absorption and measurement of Extended X-ray Absorption Fine Structure (EXAFS) spectra at a time, 5 eV-step in region of 11364-11514 eV, 1 eV-step in 11514-11554 eV, 0.25 eV-step in 11554-11594 eV, 0.03 *k*-step in 11594-12104 eV, and 0.04 *k*-step in 12104-12564 eV. Pre-edge absorption due to the background and detector were subtracted using a linear fit to the data in the range of -200 to -60 eV relative to E_0. E_0 was defined as the first inflection point on the rising absorption edge. Each spectrum was then normalized by a constant, extrapolated value to E_0 of third-order polynomial fit over absorption at 150-900 eV relative to E_0. The data analysis package used for EXAFS was the University of Washington's data analysis program. The EXAFS spectra were first subjected to background removal by fitting the pre-edge data to a Victoreen type formula over the range of -200 to 80 eV below the edge, followed by extrapolation over the energy range of interest and subtraction from the data. After the removal of the background contributions, the spectra were corrected for edge-shifts using the second derivatives of the inflection points of the data from the reference channel. The procedures used for normalization were the conventional ones. The normalization value was chosen as the absorbance at the inflection point of one EXAFS oscillation.

Table S2. Results of model fitting of k^3-weighted and Fourier-filtered Pt L_{III} EXAFS for Pd@Pt.

Sample	Bond	N	R (Å)	σ^2 (Å^2)	R_{factor} (%)
Pt/C (J.M.)	Pt-O	1.3	2.03	0.0033	0.7
	Pt-Pd	N/A	N/A	N/A	
	Pt-Pt	6.5	2.75	0.0066	
PdPd/C alloy NPs	Pt-O	1.1	1.95	0.0033*	0.8
	Pt-Pd	2.1	2.71	0.0067	
	Pt-Pt	3.0	2.69	0.0067	
Pd@Pt/C Core-shell NPs	Pt-O	1.2	2.00	0.0033*	0.3
	Pt-Pd	1.1	2.73	0.0071	
	Pt-Pt	6.5	2.74	0.0071	

2. Electrochemical analysis using a rotating disk electrode

The catalyst ink was prepared by mixing 10 mg of carbon supported nanoparticles with 50 µL of DI water, 100 µL of nafion as a binder material, and 1mL of isopropyl alcohol. Follow mixing and ultrasonification, 7µL of ink slurry was pipetted onto a glassy carbon substrate. The dried electrode was then transferred to the electrochemical cell for electrochemical measurements. Cyclic voltammetry (CV) and linear sweep volatammetry (LSV) were performed using an Autolab PGSTAT20 potentiostat and a rotating disk electrode (RDE) system (Pine) in a standard three-electrode configuration. An deposited glassy carbon electrode with a diameter of 5 mm was used as the working electrode and a platinum wire was used as the counter electrode. All the electrochemical measurements, except for the ORR with the RDE configuration, were performed in an Ar-purged 0.1 M $HClO_4$ solution. For the ORR experiment, 99.99 % oxygen gas was bubbled into the electrolyte for 30 min before each measurement respectively. Before each measurement, the glassy carbon electrode was polished with a 0.05-µm alumina paste followed by washing with distilled (DI) water in an ultrasonic bath. A saturated calomel electrode (SCE) with 3 M KCl (Gamry) and Pt mesh were used as the reference and counter electrodes, respectively. However, in this paper, all the potentials reported are with respect to the Reversible Hydrogen Electrode (RHE).

The ORR measurements were performed in 0.1 M $HClO_4$ solutions under flow of O_2 (research grade) using the glassy carbon rotating disk electrode (RDE) at a rotation rate of 1600 rpm and a sweep rate of 10 mV s^{-1}. In order to produce a clean electrode surface, several potential sweeps between 0.05 and 1.1 V versus RHE were applied to the electrode prior to the ORR measurement. In the ORR polarization curve, current densities were normalized in reference to the geometric area of the glassy carbon RDE (0.196 cm^2).

For the ORR at a RDE, the Koutecky-Levich equation can be described as follows:

$$1 / i = 1 / i_k + 1 / i_d = 1 / i_k + 1 / (0.62nFAD_0^{2/3}\omega^{1/2}v^{-1/6}C_0^*) \quad (1)$$

where i is the experimentally measured current, i_d is the diffusion-limiting current, and i_k is the kinetic current; where D_0 is the diffusivity of oxygen in 0.1 M $HClO_4$ (estimated from the product of O_2 diffusivity at infinite dilution and the ratio of the dynamic viscosities of the electrolyte and pure water), n is the number of electrons in the O_2 reduction reaction (*i.e.*, n = 4), ν is the kinematic viscosity of the electrolyte, c_0 is the solubility of O_2 in 0. 1 M $HClO_4$, and ω is the rotation rate. Then, the kinetic current was calculated based on the following equation:

$$i_k = (i \times i_d) / (i_d - i) \quad \text{---------- (2)}$$

Here, i_k is the kinetic current and i_d is the current of diffusion in the electrolyte. The diffusion current, i.e. the current that is determined by the rate of supply of dissolved hydrogen to the surface, was calculated with the Levich equation:

$$i_d = 0.62nFD^{2/3}v^{-1/6} C_0\omega^{0.5} \quad \text{---------- (3)}$$

Here, n is the number of electrons, F is Faraday's constant, D is the diffusion coefficient for hydrogen in the electrolyte, v is the kinematic viscosity of the electrolyte, c_0 is the oxygen concentration in the electrolyte, and ω is the electrode rotation rate. C_0, v, and D were calculated based on Henry's law, the method reported in reference, and the Stokes-Einstein equation, respectively. Then, given (3), formula (2) assumes the form of the following equation:

$$1/i = 1/i_k + 1/(Bc_0\omega^{0.5}) \quad \text{---------- (4)}$$

3. Single Cell Operation

40 wt % Johnson-Matthey Pt/C and prepared core@shell electrocatalysts were used as cathode catalysts for the preparation of Pt/C MEA, PdPt/C MEA, and Pd@Pt/C MEA, respectively. Catalyst ink was prepared ultrasonically using carbon-supported Pt, ally powder, and core-shell powder and ionomers (5 wt % Nafion solution, Aldrich) in a mixture of isopropyl alcohol in deionized water as a solvent. Then, prepared catalyst ink was directly coated onto the fixed membrane by spraying method. The type of membrane used in the fuel cell MEA is Nafion 211® membrane (25.4 μ m thick, DuPont™). The active area of the MEA was 10 cm^2 and 0.3 mg/cm^2 of Pt (with JM Pt/C) was loaded onto the anode and 0.3 mg/cm^2 of Pt onto cathode. The MEA was comprised of a single cell (CNL-PEM005-01, CNL Energy) with gas diffusion microporous layers, and the single-cell was connected to a fuel cell test station (CNL Energy) in order to evaluate performance and degradation in a simulated mode. Humidified hydrogen and air were fed to the anode and cathode sides of the single cell at a temperature of 75/70 ◦C. Then, the temperature and pressure of the single cell were maintained at 65 ◦C and ambient pressure during the operation. To investigate the fuel cell performance, polarization curves were obtained using a fuel cell test station for each MEA.

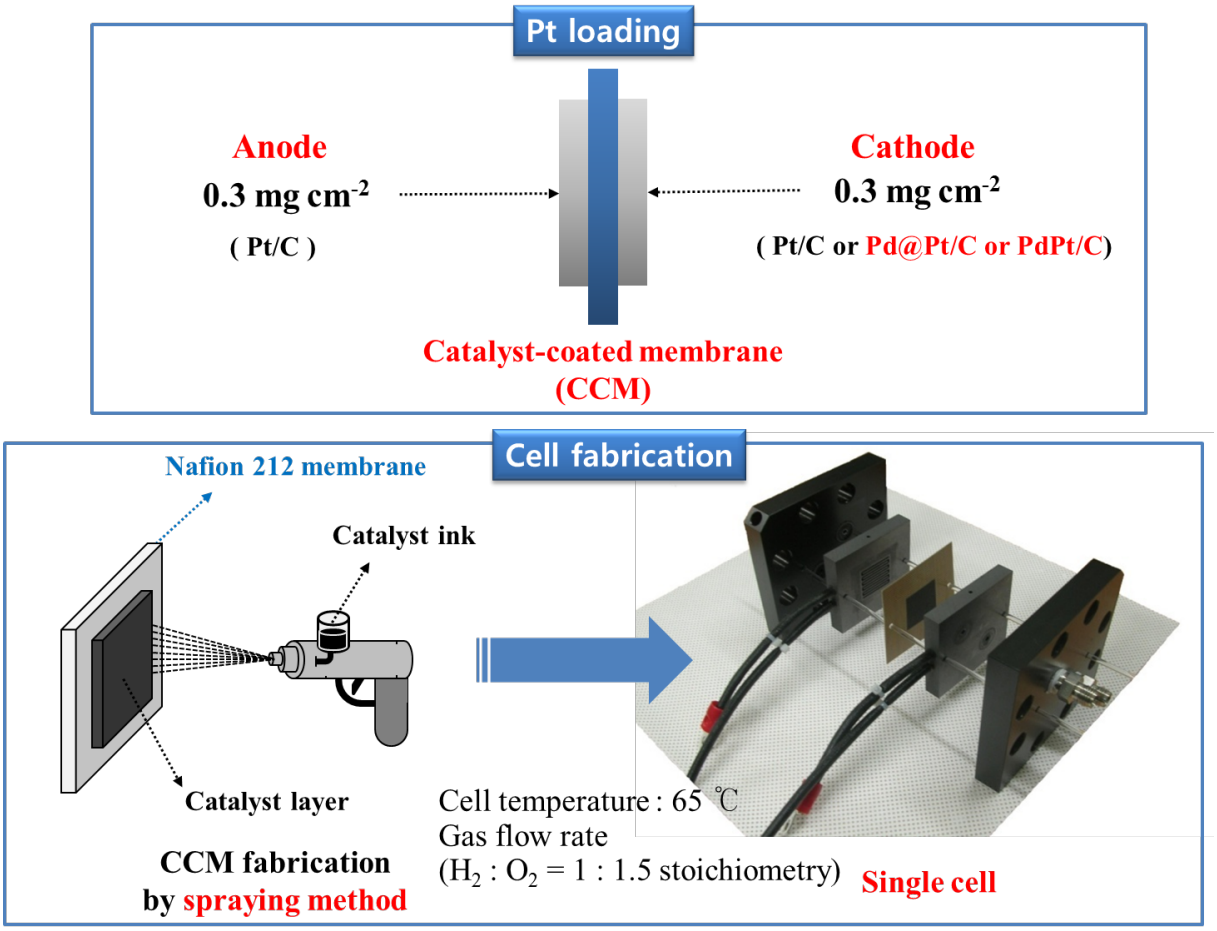

Fig. S5. Brief description of preparation process of MEA by catalyst-coated membrane (CCM) spray method.

4. Computation method using DFT calculation

4.1 Computational Detail:

- VASP: the first principle calculation program by using a planewave basis set and pseudopotential method.
- Projector augmented wave (PAW) potential
- Exchange-correlation (XC) functional: Generalized gradient approximation (GGA) by Perdew-Burke-Ernzerhof (PBE)
- Cut off energy : 400 eV
- Non-spin polarized calculation: Pt/Pd (-0.009 eV), Pt/Ir (same), and Pt (same)
  - For these materials systems, spin polarized and non-spin polarized calculations gave the same energies or very small differences as the value in parenthesis.
- Spin collinear calculation
  - Lower energy as the value in parenthesis than that of non-spin polarized calculation
- Brillouin zone sampling: 7x7x1 k-points grids based on gamma-centered point.

4.2 Model:

- Calculation of adsorption energies (E_{ad}) and vacancy formation energies (E_{vac}) for Pt skin on various sublayers
  - Pure metal sublayer: Pt/Ni, Pt/Co, Pt/Fe, Pt/Pd, Pt/Ir and Pt
- Crystal structure: face-center cubic (FCC) structure
- Lattice constants for slab models: values obtained by bulk calculation for each elements
  - Numbers in parenthesis are experimental values and the differences (%) with reference to the experiments.
  - Bulk Ni: 3.52 Å (3.52 Å, 0.0 %)
  - Bulk Co: 2.50 Å (2.50 Å, 0.0 %)

- Bulk Fe: 2.89 Å (2.86 Å, +1.0 %)
- Bulk Pd: 3.95 Å (3.89 Å, +1.5 %)
- Bulk Ir: 3.88 Å (3.84 Å, +1.0 %)

- Slab models: total eight atomic layers and the bottom two layers were fixed during relaxation.
  - Pt shell thickness: thickness of Pt layers has been changed from one to four atomic layers while total number of layers was fixed to eight.
  - Vacuum thickness: 20 Å

- Vacancy formation energy (E_{vac})
  - This energy can be used as a measure of stability of Pt surface. This is related to the bond strength of Pt atoms in Pt surface.
    - Surface stability: calculation of energy difference as a Pt atom separate from the surface
    - Single point calculation with increasing distance between the separated Pt atom and the surface
    - Maximal energy difference = vacancy formation energy (E_{vac})
  - $E_{vac} = E_{total}^{N,clean} - \left(E_{total}^{N-1} + E_{total}^{Atom}\right)$
    - N: the number of total atoms in the slab model

- Adsorption energy (E_{ad})
  - $E^{ad} = E_{total}(O-Pt/M) - 1/2E_{total}(O_2)$
  - Eight symmetrically distinct adsorption sites of O on Pt/M (M=Ir, Ni, Co, Fe, Pd)

5. ICP-AES

The prepared PdPt/C alloy NPs and Pd@Pt/C core-shell NPs samples also were measured using Optima-4300 DV (Perkin-Elmer). The resulting loading of Pt or all metals are also calculated on the basis of these ICP-AES results. ICP-AES shows higher accuracy for measuring the atomic ratio of transition metals, as compared to the other techniques such as energy dispersive spectroscopy (EDS).

Table S3. ICP-AES results of PdPt/C alloy NPs and Pd@Pt/C core-shell NPs.

nominal value	carbon-supported Pd-Pt core-shell nanoparticles		
	[Pt]/[Pd] (at %)	Pt loading (wt %)	total metal loading (wt %)
PdPt/C alloy	98.6	13.1	20.3
Pd@Pt/C core-shell	97.9	12.7	19.8

6. Confirmation of the electrochemically active surface area

The CO-stripping measurement was used to estimate the real surface area of the electrodes, following the procedures. The 0.1 M $HClO_4$ solution was purged with Ar gas for 30 min prior to electrochemical measurements. For CO-stripping measurements, pure CO was bubbled into the electrolyte under potential control at 0.1 V vs. NHE for 30 min. Then, the electrolyte was purged for 30 min with Ar gas, while keeping the electrode potential at 0.1 V vs. NHE to eliminate the dissolved CO in the electrolyte. The first anodic scan (scan speed: 10 mV s^{-1}) was performed to electro-oxidize the adsorbed CO and the subsequent voltammetries in order to verify the completeness of the CO oxidation. Assuming that each Pt surface atom is covered by a single adsorbed CO molecule, the charge for electro-desorption of CO should be 420 μC cm^{-2}. Figure 4(a) shows the voltammograms of Pt/C JM, Pd@Pt/C core-shell, and PdPt/C alloy samples in the presence and the absence of CO. The integrated CO stripping charge for all voltammograms of Pt/C JM, Pd@Pt/C core-shell, and PdPt/C alloy samples came to 243.5 μC, 268.2 μC, and 196.4 μC, respectively.

Table S4. Electrochemically active surface area results of Pt/C alloy NPs, PdPt/C alloy NPs, and Pd@Pt/C core-shell NPs.

Samples	Q_{CO} (mC/mg)	ECA(Q_{CO}) (m^2/g)
Pt/C	243.5	57.9
PdPt/C alloy	268.2	63.8
Pd@Pt/C core-shell	196.4	46.7

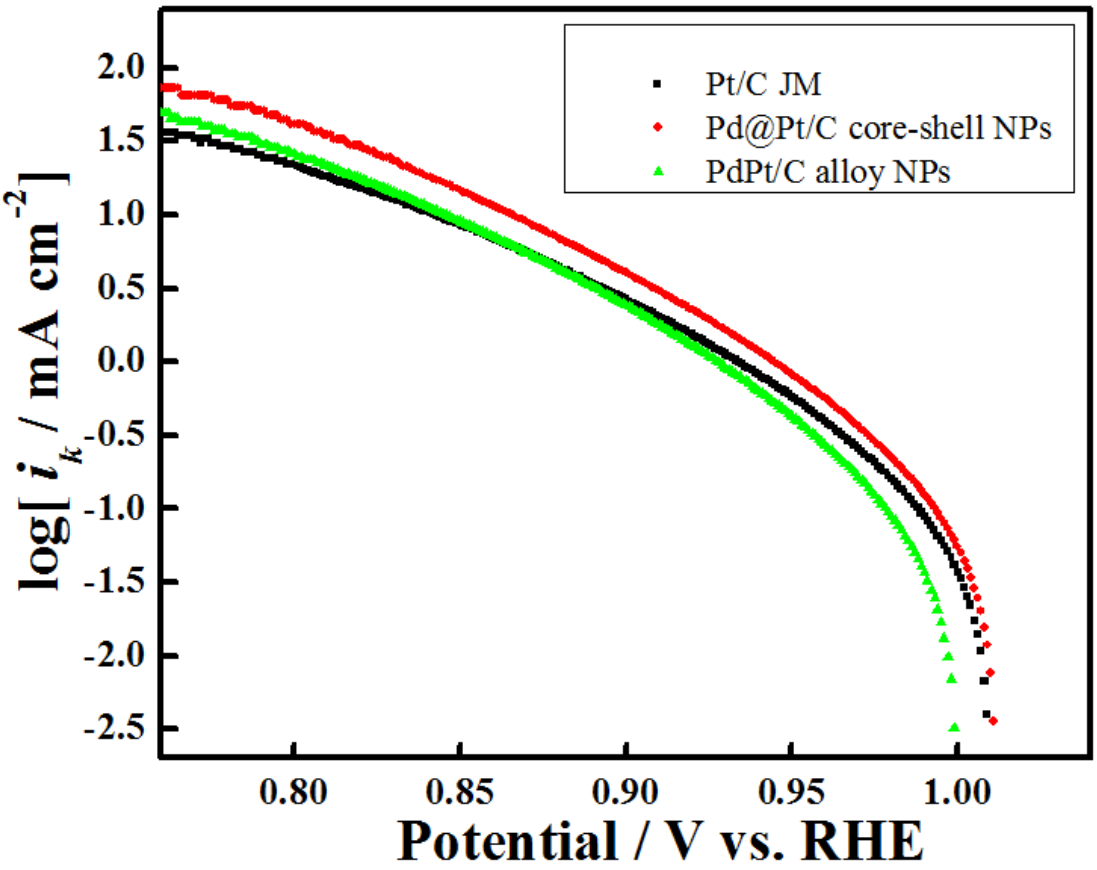

Fig. S5. Specific activity as a function of the electrode potential, V, for Pt/C alloy NPs, PdPt/C alloy NPs, and Pd@Pt/C core-shell NPs, expressed as a kinetic current density, i_k.

Table S5. Exchange current density results of Pt/C alloy NPs, PdPt/C alloy NPs, and Pd@Pt/C core-shell NPs.

Samples	i_o (mA cm^{-2})
Pt/C	3.25 x 10^{-4}
PdPt/C alloy	4.45 x 10^{-4}
Pd@Pt/C core-shell	8.01 x 10^{-4}